HHS Public Access

Author manuscript

J Hypertens. Author manuscript; available in PMC 2023 March 01.

Published in final edited form as:

J Hypertens. 2022 March 01; 40(3): 498–511. doi:10.1097/HJH.0000000000003038.

Blockade of 20-HETE Receptor Lowers Blood Pressure and Alters Vascular Function in Mice with Smooth Muscle-Specific Overexpression of CYP4A12-20-HETE Synthase

Kevin Agostinucci[a], **Rebecca Hutcheson**[a], **Sakib Hossain**[a], **Jonathan V. Pascale**[a], **Elizabeth Villegas**[a], **Frank Zhang**[a], **Adeniyi Michael Adebesin**[b], **John R. Falck**[b], **Sachin Gupte**[a], **Victor Garcia**[a], **Michal Laniado Schwartzman**[a,*]

[a]Department of Pharmacology, New York Medical College School of Medicine, Valhalla, NY 10595

[b]Department of Biochemistry, University of Texas Southwestern Medical Center, Dallas, TX 75390

Abstract

Objective: 20-Hydroxyeicosatetraenoic acid (20-HETE) is a vasoactive eicosanoid exhibiting effects on vascular smooth muscle cell (VSMC) via G-protein coupled receptor 75 (GPR75) and include stimulation of contractility, migration, and growth. We examined whether VSMC-targeted overexpression of CYP4A12, the primary 20-HETE producing enzyme in mice, is sufficient to promote hypertension.

Methods: Mice with VSM-specific *Cyp4a12* overexpression (*Myh11-4a12*) and their littermate controls (WT) were generated by crossbreeding *Cyp4a12*-floxed with *Myh11*-Cre mice. The 20-HETE receptor blocker, N-disodium succinate-20-hydroxyeicosa-6(Z),15(Z)-diencarboxamide (AAA), was administered in the drinking water. Experiments were carried out for 12 days. Systolic blood pressure was measured by tail cuff. Renal interlobar and mesenteric arteries were harvested for assessment of gene expression, 20-HETE levels, vascular contractility, vasodilation, and remodeling.

Results: Vascular and circulatory levels of 20-HETE were several folds higher in *Myh11-4a12* mice compared to WT. The *Myh11-4a12* mice compared to WT were hypertensive (145±2 vs. 127±2 mmHg; $p<0.05$) and their vasculature displayed a contractile phenotype exemplified by increased contractility, reduced vasodilatory capacity, and increased media to lumen ratio. All these features were reversed by the administration of AAA. The mechanism of increased contractility includes, at least in part, Rho-kinase activation followed by increased myosin light chain phosphorylation and activation of the contractile apparatus.

Conclusion: VSM-specific *Cyp4a12* overexpression is sufficient to alter VSM cell phenotype through changes in contractile markers and enhancement in contractility that promote hypertension and vascular dysfunction in a 20-HETE-dependent manner. The 20-HETE receptor

[*]**Corresponding Author:** Michal L. Schwartzman, Department of Pharmacology, New York Medical College, 15 Dana Road, Valhalla, NY 10595. Michal_Schwartzman@nymc.edu. Phone: +1-914-594-3116. Fax: +1-914-347-4956.

Conflict of Interest: None Disclaimers

GPR75 may represent a novel target for the treatment of hypertension and associated vascular conditions.

Keywords

20-HETE; GPR75; Hypertension; contractility; remodeling

INTRODUCTION

20-Hydroxy-5,8,11,14-eicosatetraenoic acid (20-HETE) is the ω-hydroxylation product of arachidonic acid formed by cytochrome P450 enzymes of the 4 family (CYP4A/4F). 20-HETE is a vasoactive eicosanoid that exerts its actions in conduit and resistant vessels and contributes to the regulation of blood pressure [1, 2]. Recent studies by Garcia and colleagues identified the G-protein coupled receptor GPR75 as a 20-HETE receptor (20HR) demonstrating that 20-HETE binds to and triggers a signaling cascade that culminates with changes in endothelial and smooth muscle functions [3, 4].

The primary site of 20-HETE synthesis within blood vessels is the vascular smooth muscle cell (VSMC) [5, 6]. 20-HETE can also be produced in endothelial cells (EC) [7–9] and circulating factors such as endothelial progenitor cells, platelets, and myeloid cells [7, 10, 11]. Elevated 20-HETE has been shown to increase blood pressure by changing the vessel's contractile properties. The actions of 20-HETE within the VSMC are to enhance signaling mechanisms which result in contraction. It promotes the activation of protein kinase C which phosphorylates tyrosine residues on the calcium-dependent potassium channel (BK_{Ca}^{2+}), preventing repolarization of the cell [3, 12–14]. 20-HETE has also been shown to increase Rho-kinase (ROCK) activity and increase phosphorylation of myosin light chain (MLC) at serine 19 [15] facilitating the sensitization of vessels to constrictor stimuli such as endothelin and phenylephrine [16, 17]. In addition, 20-HETE has been shown to promote endothelial dysfunction; it reduces nitric oxide (NO) bioavailability by inhibiting endothelial nitric oxide synthase (eNOS) activity [18–20] and increasing reactive oxygen species (ROS) generation that may sequester NO away from the VSMC [21, 22]. Moreover, 20-HETE induces the expression and activity of the endothelial angiotensin converting enzyme (ACE) which also contributes to endothelial dysfunction and vascular contractility [23, 24].

In addition to changes in vascular dynamics, elevated 20-HETE has been associated with remodeling of the vasculature resulting in increased vascular wall thickness [23, 25]. Remodeling of the vessel wall facilitates and exacerbates the increase in blood pressure by reducing compliance and blood flow. 20-HETE has been shown to increase migration [26] and proliferation [27–29] of VSMC. Furthermore, 20-HETE has been associated with increase in elastin degradation by increasing expression of metalloproteases [30].

The actions of 20-HETE across the vasculature have been extensively demonstrated in animal models of global overexpression of CYP4A-20-HETE synthases [31–36]. However, using global models of 20-HETE production cannot isolate 20-HETE actions within specific cell types that contribute to hypertension. In this report, a mouse model with VSMC-specific overexpression of *Cyp4a12*, the primary 20-HETE producing enzyme in mice [37], was used to determine if VSMC-specific 20-HETE promotes elevations in blood pressure and vascular

dysfunction. We hypothesize that specific overexpression of 20-HETE in the VSMC is capable of increasing blood pressure and impairing vascular function which can be reversed with administration of a 20-HETE receptor blocker (20HRB).

METHODS

Animals:

All experimental protocols were approved by the Institutional Animal Care and Use Committee in accordance with the National Institutes of Health Guidelines for the Care and Use of Laboratory Animals. Mice with VSMC-specific overexpression of *Cyp4a12* were generated by crossing mice with cre-recombinase expression driven by the VSMC-specific myosin heavy chain promoter (*Myh11-Cre*$^{+/-}$) and Cyp4a12-flox mice (*Cyp4a12*$^{fl/fl}$). *Myh11-Cre*$^{+/-}$ mice were obtained from Jackson Laboratory (stock#: 007742). The *Cyp4a12*$^{fl/fl}$ mice were generously gifted by Dr. Wolf-Hagen Schunck and Prof. Michael Bader (Max-Delbrück-Centrum, Berlin, Germany). Mice with VSMC-specific overexpression of *Cyp4a12* (*Myh11-4a12: Myh11-Cre*$^{+/-}$*Cyp4a12*$^{fl/wt}$) and corresponding wild types (WT: *Myh11-Cre*$^{-/-}$*Cyp4a12-flox*$^{fl/wt}$) began experiments at 8-12 weeks of age. All mice were housed in static cages and fed standard chow. Both male and female mice were used in this study as they exhibited similar phenotypic changes with respect to *Cyp4a12* overexpression, blood pressure and vascular function and remodeling. A water-soluble 20-HETE receptor antagonist, N-disodium succinate-20-hydroxyeicosa-6(Z),15(Z)-diencarboxamide (AAA), was used to assess the contribution of 20-HETE to the phenotype of these mice [4, 38, 39]. AAA was administered to the mice, via the drinking water (vehicle), at a dose of 10mg.kg^{-1}.day^{-1}. This dose was used because it was sufficient to lower systolic blood pressure in previous reports [39, 40]. Mice were divided into three groups: 1) WT; 2) *Myh11-4a12*; and 3) *Myh11-4a12* – AAA treatment. All groups underwent 12 days of treatment administration before tissue harvest for *ex vivo* and molecular studies.

Blood Pressure:

Systolic blood pressure was measured using CODA non-invasive tail-cuff method (Kent Scientific, Torrington, CT). The CODA tail-cuff system utilizes volume-pressure recording technology to measure the expansion of the mouse's tail due to the return of blood flow after occlusion. A warming plate was set to 32-35° Celsius to maintain body temperature during the measurement. All mice were allowed 5-7 days to acclimate to the tail-cuff procedure. The CODA system measures systolic blood pressure within ±10% of actual value. Baseline measurements per mouse were obtained by taking the average on three separate days. Once a stable blood pressure measurement was obtained, 12-day treatments began. Blood pressure measurements of mice on AAA or vehicle were measured on days 0, 4, 8, and 12.

20-HETE Measurements:

20-HETE was quantified by LC-MS/MS-based lipidomics. Blood was withdrawn at the end of the experiment by aspiration from the inferior vena cava into a heparinized syringe. Urine and plasma samples were mixed with 2 volumes of cold methanol, internal standards were added and samples kept at −80°C. Renal preglomerular arteries and mesenteric arteries were microdissected and incubated in Kreb's bicarbonate buffer, pH 7, 1 mM NADPH

at 37°C for 1 h. Tissue incubations were terminated with 2 volumes of cold methanol, internal standards were added, and samples were kept at −80°C. 20-HETE was extracted and levels quantified by LC-MS/MS on a Shimadzu Triple Quadrupole Mass Spectrometer LCMS-8050 as previously described. [41, 42]

Reverse Transcription Polymerase Chain Reaction:

Mesenteric arteries and renal interlobar arteries (RIA) were dissected and flash frozen in liquid nitrogen and stored at −80°C. Messenger RNA was obtained using the miRNeasy micro kit (Qiagen – cat#: 217084). Equal amounts of RNA were used to generate cDNA using the Quantitech cDNA synthesis kit (Qiagen – cat#: 205311). Taqman primer/probes for *Cyp4a12* (Mm00514494_m1), *Myh11* (Mm00443013_m1), Transgelin/Sm22a, *Tagln* (Mm00441661_g1), *Acta2* (Mm00725412_s1); Collagen 4a4, *Col4a4* (Mm00801574_m1); Collagen 1a1, *Col1a1* (Mm00801666_g1), and α-tubulin, *Tuba1a* (Mm00846967_g1) were purchased from Thermo Fisher Scientific. For all reactions, 2 μl cDNA was mixed in 18 μl of master mix containing: 1 μl of 20X primer/probe, 10 μl 2X Taqman advance fast master mix (Applied Biosystems – cat#: 4444557) and 7 μl nuclease free water. The thermal profile for qPCR reaction was: 50°C for 2 minutes, 95°C for 20 seconds and 40 cycles of 95°C for 3 seconds and 60°C for 30 seconds. Relative expression was calculated using the $2^{(-\Delta\Delta Ct)}$ method with expression being normalized relative to *Tuba1a*.

Western blots:

Mesenteric arteries were taken out and carefully dissected in ice-cold MOPS buffer to remove adventitia. Vessels were flash-frozen in liquid nitrogen and stored at −80°C. Tissues were lysed by crushing vessels in liquid nitrogen followed by homogenization in RIPA buffer containing protease and phosphatase inhibitor. Lysates were spun at 10,000 RPM for 15 minutes at 4°C and supernatant was collected for western blot experiments. Protein estimation was performed using BCA assay. Equal amounts of protein were loaded onto a 10%-polyacrylamide gel and ran at 125V. Proteins were transferred onto a PVDF membrane using methanol-glycine-tris-base transfer buffer. After transfer, membranes were blocked in TBS buffer containing 1% bovine serum albumin for 1 hour. Antibodies against CYP4A (1:1000 – Santa Cruz – cat#: sc-271983), ROCK1 (1:1000 – Sigma – cat#: HPA007567), Serine 1177 p-eNOS (1:100 – Cell Signaling Technology – cat#: 9571S), total eNOS (1:100 - BD Bioscience – cat#: 610297), β-Tubulin (1:2000 - Invitrogen - cat#: MA5-16308) and β-actin (1:5000 - Cell Signaling Technology – cat#: 4967) were diluted in 1% casein/TBST solution. Membranes were submerged in the antibody solution overnight on a shaker at 4°C. Secondary antibodies (Li-Cor Biotechnology) were diluted (1:15,000) in 1% casein/TBST solution and membranes were allowed to incubate for 2 hours at room temperature on a shaker. Membranes were visualized on the Li-Cor Odyssey Clx membrane scanner and quantified using ImageStudio software version 5.2.5. All western blots were represented as a Fold change compared to wild type.

Phospho-myosin light chain western blot:

The protocol for phospho-myosin light chain western blotting was based on the report of Ozaki and colleagues (1991) with modifications (29). Vessels were dissected then placed in 5% trichloroacetic acid/acetone solution and immediately placed in a −80°C freezer until

time to homogenize tissue. On the day of tissue homogenization, vessels were taken out of the freezer and allowed to thaw at room temperature for 30 minutes. After 30 minutes, vessels were moved into a 100% acetone solution and sat at room temperature for 30 minutes. Vessels were homogenized in a solution containing: 8M urea, 20mM tris-base, 22mM glycine, 10mM DTT, 5mM EGTA, 5mM Na_2EDTA. Samples were spun at 10,000 RPM for 15 minutes at room temperature. The supernatant was collected, and an equal volume was mixed with Lamelli sample buffer and loaded onto a 12% PAGE gel. The PAGE gel was transferred overnight onto a PVDF membrane in a methanol-glycine-tris-base transfer buffer. The next day, membranes were taken out and blocked in 1% BSA in TBS. Phospho-myosin light chain (pMLC, Cell Signaling Technology - cat#: 3674S) or total myosin light chain (MLC, 1:250 - Cell Signaling Technology - cat#: 3672S) was diluted in 1% casein/TBST solution (1:250) and incubated overnight at 4°C. The next day, membranes were incubated in Li-Cor secondary antibody (1:15,000) in 1% casein/TBST buffer for 2 hours. The visualization of the protein bands and the quantification were done as described above.

Wired Myography:

Phenylephrine-induced contraction, as well as acetylcholine and sodium nitroprusside (SNP) induced relaxation were performed on RIA. Kidneys were taken out of mice and were carefully dissected in a dish containing Kreb's buffer. Isolated vessels (2/mouse) were mounted onto wires in a chamber of a multivessel myograph. Before conducting experiments, vessels were allowed to sit in a bath containing Kreb's buffer, maintained at 37°C, and constantly being bubbled with 95/5% O_2/CO_2 for 30-60 minutes. All vessels were set to an internal circumference that is 90% of what the circumference would be at 100mmHg. Isometric tension was measured throughout the experiment. Cumulative phenylephrine dose-response experiments were performed. Phenylephrine was administered at half-dose intervals from (10^{-9}-10^{-4} M) directly into the tissue bath. Tension was represented as a percentage of the maximal response to 10^{-4} M phenylephrine. Acetylcholine or SNP relaxation experiments were also performed. Before acetylcholine or SNP administration, precontraction was achieved by administering phenylephrine (10^{-6} M) to the vessel bath. Acetylcholine (10^{-8}-10^{-4} M) or SNP (10^{-9}-10^{-5} M) was administered in a cumulative dose-dependent fashion after phenylephrine induced precontraction. The percent relaxation was calculated by subtracting the tension after a dose of acetylcholine or SNP from the tension generated from 10^{-6} M phenylephrine, divided by the difference between the baseline tension and 10^{-6} M phenylephrine. Percent relaxation % = [(tension at a dose of acethylcholine or SNP [M] - tension at [10^{-6} M] phenylephrine)/(tension at [10^{-6} M] phenylephrine - baseline tension)*100].

Pressure Myography:

Renal interlobar arteries were dissected in the same manner as for wired myography experiments. Living Systems Instrumentations (St. Albans City, VT) pressure myograph was used to induce pressures within the lumen of the vessel. The distances of the inner and outer diameters were measured using video edge detection. One end of the RIA was mounted onto a glass canula and the other side was ligated closed. The vessel was allowed to equilibrate for one hour at 37°C in Kreb's buffer bubbled with 95/5% O_2/CO_2. For measurements

of vascular wall thickness, internal pressures of 100mmHg were induced on normotensive vessels and 140mmHg on hypertensive vessels. Measurements of outer diameter (OD) and inner diameter (ID) under passive conditions were used to calculate media thickness [(OD - ID)/2], media:lumen ratio [(OD - ID)/ID], and medial cross-sectional area [CSA (π/4) x (OD2 - ID2)]. For measurements of the myogenic response, only WT vessels were used. Each vessel underwent 5 consecutive treatments in the following order: 1) vehicle only (100% ethanol), 2) 20-HETE (10 μM), 3) 20-HETE + AAA (10 μM), 4) 20-HETE + ROCK inhibitor (Y-27632, 10 μM), and 5) 20-HETE + AAA + Y-27632. Passive stretch of vessels was also assessed immediately after the treatments by measuring the internal diameter of the vessel in a calcium-free Kreb's solution. Vessels were subjected to pressures of 0, 20, 40, 60, 80 and 100 mmHg and ID was measured at each pressure. The absolute and normalized ID were determined after experiments were concluded. The normalized ID was represented as a percentage and calculated as follows: normalized ID = (absolute ID/passive ID)*100.

Statistics:

All values are represented as mean ± SEM. Statistical analysis was performed on GraphPad Prism 9 (version 9.2.0). Two-tailed unpaired student t-test was used to determine significance between two groups. One-way ANOVA with Tukey post-hoc test was used to compare differences between three or more means. EC_{50} from phenylephrine cumulative dose response and R_{max} for acetylcholine and SNP cumulative dose response curves were calculated and were compared using one-way ANOVA with Tukey post-hoc test. p-values <0.05 considered to be statistically significant.

RESULTS

We did not find significant quantitative or qualitative sex-differences; both male and female Myh11-4a12 mice displayed the same hypertensive phenotype when compared to corresponding WT. Therefore, we combined the results for males and females, and the numbers in the figure legends represent the total number of animals used.

Myh11-4a12 mice display elevated *Cyp4a12* expression and 20-HETE levels in blood vessels.

Cyp4a12 mRNA levels in mesenteric and renal interlobar arteries (RIA) were 5-6-fold higher in *Myh11-4a12* mice as compared to wild type mice (Figure 1A–B). There were no significant differences in vascular overexpression of *Cyp4a12* between male and female *Myh11-4a12* mice. *Cyp4a12* mRNA levels were also measured in liver and no differences were observed between the two genotypes (Figure 1C). The vascular expression of the newly identified 20-HETE receptor, GPR75, was not significantly different between the two genotypes (Figure 1D). CYP4A Protein expression was also significantly elevated in mesenteric arteries of *Myh11-4a12* mice compared to wild type mice (Figure 1E). No differences in CYP4A protein levels were observed in livers between Myh11-4a12 and wild type mice (Figure 1F).

The significant increases in *Cyp4a12* mRNA and CYP4A protein levels in arteries from *Myh11-4a12* mice were accompanied by marked increases in 20-HETE levels. As seen in

Figure 2A–B, 20-HETE levels were 6.1- and 7.7-fold higher in mesenteric and interlobar arteries, respectively, from *Myh11-4a12* mice compared to wild type mice. Moreover, 20-HETE levels were about 2-fold higher in plasma of *Myh11-4a12* mice compared to wild type (Figure 2C), while urinary levels were not different between the two groups (Figure 2D).

Myh11-4a12 mice develop hypertension and vascular dysfunction in a 20-HETE-dependent manner.

Baseline systolic blood pressure was significantly elevated in both male and female *Myh11-4a12* mice compared with corresponding wild type mice (Figure 3A). Acetylcholine-induced relaxation was assessed in RIA and mice with VSMC-specific overexpression of *Cyp4a12* had less than a 50% response to acetylcholine in contrast to 80% response in wild type (Figure 3B). Renal interlobar arteries from either genotype had a similar relaxation response to SNP (Figure 3C) indicating impaired NO bioavailability rather than response to NO. Indeed, assessment of eNOS activation indicated a 50% reduction of serine 1177 phospho-eNOS expression in *Myh11-4a12* compared to wild type mice (Figure 3D). These results substantiate the notion that the impairment in acetylcholine-induced relaxation may be due to reductions in NO bioavailability. Vascular remodeling was also evident in arteries from *Myh11-4a12* mice. As seen in Figure 3E–G, media-to-lumen ratio, media thickness, and media cross-sectional area were significantly higher in *Myh11-4a12* arteries compared to wild type. Altogether, *Myh11-4a12* mice display impairments in blood pressure and vascular function at baseline compared to wild type mice.

The recent findings that binding and activation of GPR75 underlies 20-HETE-mediated hypertension and vascular dysfunction [3] provide tools, e.g., receptor blockers, to assess the contribution of 20-HETE to the observed phenotype. In this study, the elevation in blood pressure appeared to be dependent on 20-HETE since administration of the 20HRB, AAA [4], for 12 days reduced blood pressure in *Myh11-4a12* mice to levels seen in wild type mice (Figure 4A). Significant blood pressure reduction in AAA-treated *Myh11-4a12* mice was observed at the 8^{th} and 12^{th} days of treatment ($p<0.0001$). Both male and female *Myh11-4a12* mice responded to AAA treatment with a similar reduction in blood pressure (in males:147±4 to 124±2 mmHg; in females:142±3 to 126±2 mmHg). There was no significant blood pressure reduction in wild type mice treated with AAA. The changes in vascular reactivity were also dependent on 20-HETE. As seen in Figure 4B, there was a leftward shift in the phenylephrine dose-response curve and the EC_{50} value was reduced in *Myh11-4a12* mice compared to wild type mice. Treatment of *Myh11-4a12* mice with AAA shifted the dose response curve to the right and the calculated EC_{50} was not significantly different from that observed in arteries from wild type mice (Figure 4B). Similarly, arteries from *Myh11-4a12* mice on AAA (Figure 4C) had improved response to acetylcholine compared to *Myh11-4a12* on vehicle. Measurements of vascular remodeling were also assessed in RIA after 12 days of AAA treatment. The media to lumen ratio was the only parameter that was affected by AAA treatment. After 12 days of AAA administration, there was a significant reduction in the media to lumen ratio in *Myh11-4a12* mice. The media thickness and cross-sectional area were unaffected by 12 days of AAA administration (Figures 4D–4F). The measurements remained higher than wild type values

and were not significantly different than *Myh11-4a12* mice on vehicle. It should be noted that administration of AAA did not affect plasma levels of 20-HETE in *Myh11-4a12* mice (viz., 298±36 vs 297±58 pg/ml in vehicle- vs AAA-treated *Myh11-4a12* mice; n=10) which were about 2-fold higher than levels in vehicle-treated WT (157±23 pg/ml; $p<0.05$; n=10)

Vascular smooth muscle cells from *Myh11-4a12* mice exhibited a contractile phenotype

Smooth muscle markers (*Myh11, Tagln*, and *Acta2*) were measured to determine the phenotypic state the VSMC were exhibiting. *Myh11-4a12* RIA expressed almost a 2-fold increase of *Myh11* and *Tagln* compared to wild type mice (Figure 5A & 5B). *Acta2* mRNA expression was about 50% higher compared to wild type mice (Figure 5C). After 12 days of AAA treatment, all the VSMC markers remained elevated in *Myh11-4a12* mice compared to wild type mice and were not different compared to untreated *Myh11-4a12* mice (Figure 5A–5C). Collagen expression was also assessed to determine if there were any changes that can contribute to the remodeling of the extracellular matrix. Levels of *Collagen I* mRNA in RIA were significantly lower in *Myh11-4a12* mice as compared to WT mice, whereas *Collagen IV* mRNA levels were not different (Figure 5D&5E).

Myh11-4a12 display changes in cellular signaling for VSMC contraction which may be explained by changes in ROCK activity. Mesenteric arteries were assessed for myosin light chain phosphorylation to determine the downstream signaling event for smooth muscle cell contraction. *Myh11-4a12* vessels had a 60% increase in phosphorylated MLC expression compared to wild type vessels (Figure 6A). Twelve days of AAA treatment reduced the expression of phosphorylated MLC to a level similar to wild type vessels (Figure 6A). The changes in expression of phosphorylated myosin light chain may be due to change in ROCK expression and/or activity. ROCK1 protein expression was assessed and there was a 60% increase in *Myh11-4a12* RIA compared to wild type (Figure 6B), however, ROCK1 expression was not affected by 12 days of AAA treatment (data not shown). Next, ROCK activity was assessed via pressure myography. Renal interlobar arteries from wild type mice underwent pressure myography to assess 20-HETE ability to affect the myogenic response. There was a downward shift in the absolute and normalized internal diameter (ID) curves of vessels treated with 20-HETE suggesting an increase myogenic response (Figure 6C & 6D). Comparisons at 100 mmHg were made and there was a significant reduction in the absolute ID (Figure 6E) and normalized ID (Figure 6F) of 20-HETE treated vessels compared to vehicle treated vessels. Co-administration of 20-HETE with either AAA or the ROCK inhibitor Y-27632 increased the absolute and normalized ID compared to 20-HETE alone (Figures 6E & 6F). Lastly, when 20-HETE was co-administered with AAA and Y-27632, no further increases in the absolute or normalized ID were observed (Figures 6E & 6F).

DISCUSSION

Global overexpression of *Cyp4a12* and 20-HETE have been documented to promote hypertension by mechanisms that alter VSMC and endothelial cell functions. The contribution of the VSMC to 20-HETE-dependent increase in blood pressure is multifactorial including: 1) inhibition of the Calcium-dependent potassium (BK_{Ca}^{2+}) channel [3, 13]; 2) increase in Rho-kinase activity [15] and 3) promotion of vascular

remodeling [23, 25]. On the other hand, the endothelial cell component of the blood pressure elevation includes: 1) impairment of NO-mediated vasodilation [18], 2) increase endothelial ACE expression [24, 43] and 3) activation of inflammatory program [44, 45]. The limitation in using global overexpression models is that the precise mechanism cannot be isolated, within different cell types, due to the multifactorial actions of 20-HETE. This is the first report showing the contribution of VSMC-specific overexpression of *Cyp4a12* to changes in blood pressure.

The cre/lox system was utilized for site-specific overexpression of *Cyp4a12*. Cre-recombinase was directed to the VSMC by utilizing the myosin heavy chain 11 promoter [46]. This promoter was used because it is the most specific marker in smooth muscle cells [47]. The present data show that *Myh11-4a12* mice have overexpression of *Cyp4a12 mRNA* and CYP4A protein limited to the vasculature which was accompanied by increases in 20-HETE within the vessels and plasma, but not in urine, indicating the effectiveness of this targeted expression.

The *Myh11-4a12* mice displayed a mild hypertensive phenotype evidenced by systolic blood pressure of about 15 mmHg higher than its corresponding wild type mice. The hypertensive phenotype may be the consequence of increased vascular reactivity and smooth muscle hypertrophy brought about by increased vascular production of 20-HETE. Blood vessels from *Myh11-4a12* mice exhibited increased sensitivity to constrictor stimuli such as phenylephrine suggesting that increased production of 20-HETE within the VSMC acts as an autocrine mediator to stimulate the contractile apparatus. That this sensitization to constrictor stimuli was 20-HETE dependent is evident by the ability of its receptor blocker, AAA, to prevent the increased contraction to phenylephrine. We have shown that 20-HETE-GPR75 pairing results in a rapid increase in intracellular calcium and that AAA blocks the binding/pairing and the ensuing signaling cascade [3, 4]. Hence, it is reasonable to suggest that in these mice the vascular smooth muscle 20-HETE-GPR75 signaling pathway is amplified leading to increasing intracellular calcium via mechanisms that may include inhibition of BK_{Ca}^{2+} channels and activation of L-type Ca^{+2} channels and/or activation of the Rho-kinase (ROCK) leading to increased phosphorylation of MLC [12, 13, 15]. In this study, we showed that the levels of the phosphorylated MLC at serine 19 is significantly higher in blood vessels from *Myh11-4a12* mice than in corresponding WT mice and that treatment with AAA reduced its levels to that of the WT. We also showed that activation of Rho kinase mediates 20-HETE-GPR75-dependent increases in contractions.

The increased contractile phenotype in *Myh11-4a12* blood vessels is also exemplified by significant increases in the expression of this phenotype markers across the vasculature, including *Myh11*, *Tagln* and *Acta2* along with decreased expression of collagen [48]. These results coupled together with the observed increases in media thickness and cross-sectional area in *Myh11-4a12* blood vessels denote a vascular hypertrophic phenotype which goes hand in hand with the contractile phenotype. Interestingly, the expression of these contractile markers was not affected by the 12-day treatment with the 20-HETE receptor blocker. Likewise, media thickness as well as cross-sectional area were unchanged in response to AAA suggesting that in this model there is no direct effect of 20-HETE on remodeling and that hypertrophy may be a consequence of increased levels of contractile proteins.

Notably, AAA administration reduced media to lumen ratio which was significantly higher in *Myh11-4a12* blood vessels. The reason for this may be due to AAA's ability to promote expansion of the lumen, through mechanisms affecting vascular contraction, rather than changing the vascular wall structure. On the other hand, the inability of AAA to reduce media hypertrophy may be related to the short duration of its administration.

Endothelial dysfunction exemplified by impaired acetylcholine-induced relaxation was also a feature of the *Myh11-4a12* vascular phenotype that was dependent on 20-HETE-GPR75 pairing since it was reversed by AAA treatment. The demonstration of reduced phosphorylated eNOS at serine 1177 in *Myh11-4a12* blood vessels coupled with the fact that relaxations to NO donor were not different between the genotypes suggested diminished NO bioavailability. We and others have shown that 20-HETE uncouples eNOS and activate ROS production [18, 49–52]; both leading to reduction in NO bioavailability. The question here is how an increase in vascular smooth muscle cell-derived 20-HETE affects the adjacent endothelial cells. As a small lipid molecule, 20-HETE can easily cross cell membranes and act as a paracrine mediator. The finding that plasma 20-HETE levels are higher in the *Myh11-4a12* compared to WT mice suggest a directional spillover of 20-HETE from the smooth muscle through the endothelial cell layer to the circulation. To this end, Jiang et al.,[53] showed that overproduction of 20-HETE in smooth muscle stimulated endothelial cells proliferation. In contrast, Cheng et al., [44] showed that endothelial-specific expression of CYP4F2, a human 20-HETE synthase, impaired acetylcholine-induced relaxation, but did not affect smooth muscle contractility. However, although we used a specific smooth muscle promoter to create the *Myh11-4a12* mice, we cannot exclude the possibility of increased production of 20-HETE in the endothelial cells or blood cells. Such increases may be the consequence of changes in blood flow due to increased blood pressure and changes in vascular morphology. Our attempts to document overexpression of CYP4A12 protein within the smooth muscle layer failed primarily due to the unavailability of specific antibody and the difficulties in showing overexpression versus deletion with antibody that is against all CYP4A proteins.

In summary, this study demonstrates that smooth muscle-specific overexpression of *Cyp4a12* is sufficient to alter VSMC contractility through changes in phenotypic markers and enhancements in contractility that promote elevations in blood pressure and vascular remodeling. The use of a 20HRB clearly illustrates the 20HR's contribution to these changes and further highlights the 20HR as a therapeutic target for the treatment of hypertension and associated vascular dysfunction. The clinical significance of this study is exemplified by the fact that despite having an array of anti-hypertensive drugs, approximately one-third of the population which fit into the definition of hypertension (>130/80 mmHg) do not see a successful outcome from using hypertensive medications [54]. Thus, there is a need to identify new cellular mechanisms to identify novel therapeutic targets and to develop drugs to combat hypertension. 20-HETE has been associated with elevations in blood pressure in animal models and in humans [55, 56]. The effects of 20-HETE are multifaceted including changes in vascular function and changes in sodium and urine handling [57]. The use of pharmacological antagonists has demonstrated that the actions of 20-HETE can be blocked to improve blood pressure [23, 34, 58, 59]. The discovery of GPR75 as the 20-HETE

receptor provides a new and specific target to interfere with 20-HETE's actions and a novel strategy in the treatment of hypertension.

Funding:

This study was funded by NIH/NHLBI grant HL139793 (MLS), diversity supplement to Victor Garcia HL139793-1S, and by the Robert A. Welch Foundation (I-0011) (JRF).

REFERENCES

1. Garcia V, Schwartzman ML. Recent developments on the vascular effects of 20-hydroxyeicosatetraenoic acid. Curr Opin Nephrol Hypertens. 2017;26(2):74–82. Epub 2016/12/03. doi: 10.1097/mnh.0000000000000302. [PubMed: 27906746]
2. Rocic P, Schwartzman ML. 20-HETE in the regulation of vascular and cardiac function. Pharmacology & therapeutics. 2018. Epub 2018/07/27. doi: 10.1016/j.pharmthera.2018.07.004.
3. Garcia V, Gilani A, Shkolnik B, Pandey V, Zhang FF, Dakarapu R, et al. 20-HETE Signals Through G-Protein-Coupled Receptor GPR75 (Gq) to Affect Vascular Function and Trigger Hypertension. Circ Res. 2017;120(11):1776–1788. Epub 2017/03/23. doi: 10.1161/circresaha.116.310525. [PubMed: 28325781]
4. Pascale JV, Park EJ, Adebesin AM, Falck JR, Schwartzman ML, Garcia V. Uncovering the signaling, structure and function of the 20-HETE-GPR75 pairing: Identifying CCL5 as a negative regulator of GPR75. British journal of pharmacology. 2021. Epub 2021/05/12. doi: 10.1111/bph.15525.
5. Gebremedhin D, Lange AR, Narayanan J, Aebly MR, Jacobs ER, Harder DR. Cat cerebral arterial smooth muscle cells express cytochrome P450 4A2 enzyme and produce the vasoconstrictor 20-HETE which enhances L-type Ca2+ current. The Journal of physiology. 1998;507 (Pt 3):771–781. Epub 1998/05/23. [PubMed: 9508838]
6. Marji JS, Wang MH, Laniado-Schwartzman M. Cytochrome P-450 4A isoform expression and 20-HETE synthesis in renal preglomerular arteries. Am J Physiol Renal Physiol. 2002;283(1):F60–67. Epub 2002/06/13. doi: 10.1152/ajprenal.00265.2001. [PubMed: 12060587]
7. Chen L, Ackerman R, Saleh M, Gotlinger KH, Kessler M, Mendelowitz LG, et al. 20-HETE regulates the angiogenic functions of human endothelial progenitor cells and contributes to angiogenesis in vivo. J Pharmacol Exp Ther. 2014;348(3):442–451. Epub 2014/01/10. doi: 10.1124/jpet.113.210120. . [PubMed: 24403517]
8. Chen L, Tang S, Zhang FF, Garcia V, Falck JR, Schwartzman ML, et al. CYP4A/20-HETE regulates ischemia-induced neovascularization via its actions on endothelial progenitor and preexisting endothelial cells. Am J Physiol Heart Circ Physiol. 2019;316(6):H1468–h1479. Epub 2019/04/06. doi: 10.1152/ajpheart.00690.2018. [PubMed: 30951365]
9. Zhu D, Zhang C, Medhora M, Jacobs ER. CYP4A mRNA, protein, and product in rat lungs: novel localization in vascular endothelium. Journal of applied physiology (Bethesda, Md : 1985). 2002;93(1):330–337. Epub 2002/06/19. doi: 10.1152/japplphysiol.01159.2001.
10. Hill E, Murphy RC. Quantitation of 20-hydroxy-5,8,11,14-eicosatetraenoic acid (20-HETE) produced by human polymorphonuclear leukocytes using electron capture ionization gas chromatography/mass spectrometry. Biological mass spectrometry. 1992;21(5):249–253. Epub 1992/05/01. doi: 10.1002/bms.1200210505. [PubMed: 1525186]
11. Tsai IJ, Croft K, Puddey IB, Beilin LJ, Barden AE. 20-Hydroxyeicosatetraenoic Acid Synthesis Is Increased in Human Neutrophils and Platelets by Angiotensin Ii and Endothelin-1. Am J Physiol Heart Circ Physiol. 2011;300(4):H1194–1200. [PubMed: 21239640]
12. Sun CW, Falck JR, Harder DR, Roman RJ. Role of tyrosine kinase and PKC in the vasoconstrictor response to 20-HETE in renal arterioles. Hypertension. 1999;33(1 Pt 2):414–418. Epub 1999/02/04. [PubMed: 9931139]
13. Zou AP, Fleming JT, Falck JR, Jacobs ER, Gebremedhin D, Harder DR, et al. 20-HETE is an endogenous inhibitor of the large-conductance Ca(2+)-activated K+ channel in renal arterioles. Am J Physiol. 1996;270(1 Pt 2):R228–237. Epub 1996/01/01. [PubMed: 8769806]

14. Toth P, Csiszar A, Tucsek Z, Sosnowska D, Gautam T, Koller A, et al. Role of 20-HETE, TRPC channels, and BKCa in dysregulation of pressure-induced Ca2+ signaling and myogenic constriction of cerebral arteries in aged hypertensive mice. Am J Physiol Heart Circ Physiol. 2013;305(12):H1698–1708. Epub 2013/10/08. doi: 10.1152/ajpheart.00377.2013. . [PubMed: 24097425]
15. Randriamboavonjy V, Busse R, Fleming I. 20-HETE-induced contraction of small coronary arteries depends on the activation of Rho-kinase. Hypertension. 2003;41(3 Pt 2):801–806. Epub 2003/03/08. doi: 10.1161/01.hyp.0000047240.33861.6b. [PubMed: 12623999]
16. Hercule HC, Oyekan AO. Cytochrome P450 omega/omega-1 hydroxylase-derived eicosanoids contribute to endothelin(A) and endothelin(B) receptor-mediated vasoconstriction to endothelin-1 in the rat preglomerular arteriole. J Pharmacol Exp Ther. 2000;292(3):1153–1160. Epub 2000/02/25. [PubMed: 10688635]
17. Zhang F, Wang MH, Krishna UM, Falck JR, Laniado-Schwartzman M, Nasjletti A. Modulation by 20-HETE of phenylephrine-induced mesenteric artery contraction in spontaneously hypertensive and Wistar-Kyoto rats. Hypertension. 2001;38(6):1311–1315. Epub 2001/12/26. [PubMed: 11751709]
18. Cheng J, Ou JS, Singh H, Falck JR, Narsimhaswamy D, Pritchard KA Jr., et al. 20-Hydroxyeicosatetraenoic acid causes endothelial dysfunction via eNOS uncoupling. Am J Physiol Heart Circ Physiol. 2008;294(2):H1018–1026. [PubMed: 18156192]
19. Cheng J, Wu CC, Gotlinger KH, Zhang F, Falck JR, Narsimhaswamy D, et al. 20-hydroxy-5,8,11,14-eicosatetraenoic acid mediates endothelial dysfunction via IkappaB kinase-dependent endothelial nitric-oxide synthase uncoupling. J Pharmacol Exp Ther. 2010;332(1):57–65. Epub 2009/10/21. doi: 10.1124/jpet.109.159863. [PubMed: 19841472]
20. Li X, Zhao G, Ma B, Li R, Hong J, Liu S, et al. 20-Hydroxyeicosatetraenoic acid impairs endothelial insulin signaling by inducing phosphorylation of the insulin receptor substrate-1 at Ser616. PloS one. 2014;9(4):e95841. Epub 2014/04/26. doi: 10.1371/journal.pone.0095841. [PubMed: 24763529]
21. Medhora M, Chen Y, Gruenloh S, Harland D, Bodiga S, Zielonka J, et al. 20-HETE increases superoxide production and activates NAPDH oxidase in pulmonary artery endothelial cells. Am J Physiol Lung Cell Mol Physiol. 2008;294(5):L902–911. Epub 2008/02/26. doi: 10.1152/ajplung.00278.2007. [PubMed: 18296498]
22. Inoue K, Sodhi K, Puri N, Gotlinger KH, Cao J, Rezzani R, et al. Endothelial-specific CYP4A2 overexpression leads to renal injury and hypertension via increased production of 20-HETE. Am J Physiol Renal Physiol. 2009;297(4):F875–884. Epub 2009/08/14. doi: 10.1152/ajprenal.00364.2009. [PubMed: 19675180]
23. Garcia V, Joseph G, Shkolnik B, Ding Y, Zhang FF, Gotlinger K, et al. Angiotensin II receptor blockade or deletion of vascular endothelial ACE does not prevent vascular dysfunction and remodeling in 20-HETE-dependent hypertension. Am J Physiol Regul Integr Comp Physiol. 2015;309(1):R71–78. Epub 2015/05/01. doi: 10.1152/ajpregu.00039.2015. [PubMed: 25924878]
24. Garcia V, Shkolnik B, Milhau L, Falck JR, Schwartzman ML. 20-HETE Activates the Transcription of Angiotensin-Converting Enzyme via Nuclear Factor-kappaB Translocation and Promoter Binding. J Pharmacol Exp Ther. 2016;356(3):525–533. Epub 2015/12/25. doi: 10.1124/jpet.115.229377. [PubMed: 26699146]
25. Ding Y, Wu CC, Garcia V, Dimitrova I, Weidenhammer A, Joseph G, et al. 20-HETE induces remodeling of renal resistance arteries independent of blood pressure elevation in hypertension. Am J Physiol Renal Physiol. 2013;305(5):F753–763. Epub 2013/07/05. doi: 10.1152/ajprenal.00292.2013. [PubMed: 23825080]
26. Stec DE, Gannon KP, Beaird JS, Drummond HA. 20-Hydroxyeicosatetraenoic acid (20-HETE) stimulates migration of vascular smooth muscle cells. Cell Physiol Biochem. 2007;19(1–4):121–128. Epub 2007/02/21. doi: 10.1159/000099200. [PubMed: 17310106]
27. Kalyankrishna S, Malik KU. Norepinephrine-induced stimulation of p38 mitogen-activated protein kinase is mediated by arachidonic acid metabolites generated by activation of cytosolic phospholipase A(2) in vascular smooth muscle cells. J Pharmacol Exp Ther. 2003;304(2):761–772. Epub 2003/01/23. doi: 10.1124/jpet.102.040949. [PubMed: 12538832]

28. Muthalif MM, Benter IF, Karzoun N, Fatima S, Harper J, Uddin MR, et al. 20-Hydroxyeicosatetraenoic acid mediates calcium/calmodulin-dependent protein kinase II-induced mitogen-activated protein kinase activation in vascular smooth muscle cells. Proc Natl Acad Sci U S A. 1998;95(21):12701–12706. Epub 1998/10/15. [PubMed: 9770549]

29. Orozco LD, Liu H, Perkins E, Johnson DA, Chen BB, Fan F, et al. 20-Hydroxyeicosatetraenoic acid inhibition attenuates balloon injury-induced neointima formation and vascular remodeling in rat carotid arteries. J Pharmacol Exp Ther. 2013;346(1):67–74. Epub 2013/05/10. doi: 10.1124/jpet.113.203844. [PubMed: 23658377]

30. Soler A, Hunter I, Joseph G, Hutcheson R, Hutcheson B, Yang J, et al. Elevated 20-HETE in metabolic syndrome regulates arterial stiffness and systolic hypertension via MMP12 activation. Journal of molecular and cellular cardiology. 2018;117:88–99. Epub 2018/02/13. doi: 10.1016/j.yjmcc.2018.02.005. [PubMed: 29428638]

31. Singh H, Cheng J, Deng H, Kemp R, Ishizuka T, Nasjletti A, et al. Vascular cytochrome P450 4A expression and 20-hydroxyeicosatetraenoic acid synthesis contribute to endothelial dysfunction in androgen-induced hypertension. Hypertension. 2007;50(1):123–129. Epub 2007/06/06. doi: 10.1161/hypertensionaha.107.089599. [PubMed: 17548721]

32. Sodhi K, Wu CC, Cheng J, Gotlinger K, Inoue K, Goli M, et al. CYP4A2-induced hypertension is 20-hydroxyeicosatetraenoic acid- and angiotensin II-dependent. Hypertension. 2010;56(5):871–878. Epub 2010/09/15. doi: 10.1161/hypertensionaha.110.154559. [PubMed: 20837888]

33. Wu CC, Cheng J, Zhang FF, Gotlinger KH, Kelkar M, Zhang Y, et al. Androgen-dependent hypertension is mediated by 20-hydroxy-5,8,11,14-eicosatetraenoic acid-induced vascular dysfunction: role of inhibitor of kappaB Kinase. Hypertension. 2011;57(4):788–794. Epub 2011/02/16. doi: 10.1161/hypertensionaha.110.161570. [PubMed: 21321301]

34. Wu CC, Mei S, Cheng J, Ding Y, Weidenhammer A, Garcia V, et al. Androgen-sensitive hypertension associates with upregulated vascular CYP4A12-20-HETE synthase. J Am Soc Nephrol. 2013;24(8):1288–1296. Epub 2013/05/04. doi: 10.1681/asn.2012070714. [PubMed: 23641057]

35. Holla VR, Adas F, Imig JD, Zhao X, Price E Jr.,, Olsen N, et al. Alterations in the regulation of androgen-sensitive Cyp 4a monooxygenases cause hypertension. Proc Natl Acad Sci U S A. 2001;98(9):5211–5216. Epub 2001/04/26. doi: 10.1073/pnas.081627898. [PubMed: 11320253]

36. Savas U, Wei S, Hsu MH, Falck JR, Guengerich FP, Capdevila JH, et al. 20-Hydroxyeicosatetraenoic Acid (HETE)-dependent Hypertension in Human Cytochrome P450 (CYP) 4A11 Transgenic Mice: NORMALIZATION OF BLOOD PRESSURE BY SODIUM RESTRICTION, HYDROCHLOROTHIAZIDE, OR BLOCKADE OF THE TYPE 1 ANGIOTENSIN II RECEPTOR. J Biol Chem. 2016;291(32):16904–16919. Epub 2016/06/15. doi: 10.1074/jbc.M116.732297. [PubMed: 27298316]

37. Muller DN, Schmidt C, Barbosa-Sicard E, Wellner M, Gross V, Hercule H, et al. Mouse Cyp4a isoforms: enzymatic properties, gender- and strain-specific expression, and role in renal 20-hydroxyeicosatetraenoic acid formation. The Biochemical journal. 2007;403(1):109–118. Epub 2006/11/23. doi: 10.1042/bj20061328. [PubMed: 17112342]

38. Cardenas S, Colombero C, Panelo L, Dakarapu R, Falck John R, Costas Monica A, et al. GPR75 receptor mediates 20-HETE-signaling and metastatic features of androgen-insensitive prostate cancer cells. Biochimica et biophysica acta Molecular and cell biology of lipids. 2019;1865:158573–158580. Epub 2019/11/25. doi: 10.1016/j.bbalip.2019.158573. [PubMed: 31760076]

39. Walkowska A, Červenka L, Imig JD, Falck JR, Sadowski J, Kompanowska-Jezierska E. Early Renal Vasodilator and Hypotensive Action of Epoxyeicosatrienoic Acid Analog (EET-A) and 20-HETE Receptor Blocker (AAA) in Spontaneously Hypertensive Rats. Frontiers in physiology. 2021;12:622882. Epub 2021/02/16. doi: 10.3389/fphys.2021.622882. [PubMed: 33584348]

40. Sedláková L, Kikerlová S, Husková Z, Červenková L, Chábová V, Zicha J, et al. 20-Hydroxyeicosatetraenoic acid antagonist attenuates the development of malignant hypertension and reverses it once established: a study in Cyp1a1-Ren-2 transgenic rats. Bioscience reports. 2018;38(5). Epub 2018/07/29. doi: 10.1042/bsr20171496.

41. Gilani A, Agostinucci K, Pascale JV, Hossain S, Kandhi S, Pandey V, et al. Proximal tubular-targeted overexpression of the Cyp4a12-20-HETE synthase promotes salt-sensitive hypertension in

male mice. Am J Physiol Regul Integr Comp Physiol. 2020;319(1):R87–95. Epub 2020/07/08. doi: 10.1152/ajpregu.00089.2020.

42. Gilani A, Pandey V, Garcia V, Agostinucci K, Singh SP, Schragenheim J, et al. High-fat diet-induced obesity and insulin resistance in CYP4a14(−/−) mice is mediated by 20-HETE. Am J Physiol Regul Integr Comp Physiol. 2018;315(5):R934–r944. Epub 2018/08/09. doi: 10.1152/ajpregu.00125.2018. [PubMed: 30088983]
43. Cheng J, Garcia V, Ding Y, Wu CC, Thakar K, Falck JR, et al. Induction of Angiotensin-Converting Enzyme and Activation of the Renin-Angiotensin System Contribute to 20-Hydroxyeicosatetraenoic Acid-Mediated Endothelial Dysfunction. Arterioscler Thromb Vasc Biol. 2012;32(8):1917–1924. Epub 2012/06/23. doi: 10.1161/atvbaha.112.248344. [PubMed: 22723444]
44. Cheng J, Edin ML, Hoopes SL, Li H, Bradbury JA, Graves JP, et al. Vascular characterization of mice with endothelial expression of cytochrome P450 4F2. Faseb J. 2014;28(7):2915–2931. Epub 2014/03/29. doi: 10.1096/fj.13-241927. [PubMed: 24668751]
45. Ishizuka T, Cheng J, Singh H, Vitto MD, Manthati VL, Falck JR, et al. 20-Hydroxyeicosatetraenoic acid stimulates nuclear factor-kappaB activation and the production of inflammatory cytokines in human endothelial cells. J Pharmacol Exp Ther. 2008;324(1):103–110. Epub 2007/10/20. doi: 10.1124/jpet.107.130336. [PubMed: 17947496]
46. Xin HB, Deng KY, Rishniw M, Ji G, Kotlikoff MI. Smooth muscle expression of Cre recombinase and eGFP in transgenic mice. Physiological genomics. 2002;10(3):211–215. [PubMed: 12209023]
47. Chakraborty R, Saddouk FZ, Carrao AC, Krause DS, Greif DM, Martin KA. Promoters to Study Vascular Smooth Muscle. Arterioscler Thromb Vasc Biol. 2019;39(4):603–612. Epub 2019/02/08. doi: 10.1161/atvbaha.119.312449. [PubMed: 30727757]
48. Chettimada S, Joshi SR, Dhagia V, Aiezza A 2nd, Lincoln TM, Gupte R, et al. Vascular smooth muscle cell contractile protein expression is increased through protein kinase G-dependent and -independent pathways by glucose-6-phosphate dehydrogenase inhibition and deficiency. Am J Physiol Heart Circ Physiol. 2016;311(4):H904–h912. Epub 2016/08/16. doi: 10.1152/ajpheart.00335.2016. [PubMed: 27521420]
49. Joseph G, Soler A, Hutcheson R, Hunter I, Bradford C, Hutcheson B, et al. Elevated 20-HETE impairs coronary collateral growth in metabolic syndrome via endothelial dysfunction. Am J Physiol Heart Circ Physiol. 2017;312(3):H528–H540. Epub 2016/12/25. doi: 10.1152/ajpheart.00561.2016. [PubMed: 28011587]
50. Ward NC, Chen K, Li C, Croft KD, Keaney JF Jr. Chronic activation of AMP-activated protein kinase prevents 20-hydroxyeicosatetraenoic acid-induced endothelial dysfunction. Clin Exp Pharmacol Physiol. 2011;38(5):328–333. Epub 2011/03/11. doi: 10.1111/j.1440-1681.2011.05509.x. [PubMed: 21388435]
51. Zeng Q, Han Y, Bao Y, Li W, Li X, Shen X, et al. 20-HETE increases NADPH oxidase-derived ROS production and stimulates the L-type Ca2+ channel via a PKC-dependent mechanism in cardiomyocytes. Am J Physiol Heart Circ Physiol. 2010;299(4):H1109–1117. Epub 2010/08/03. doi: 10.1152/ajpheart.00067.2010. [PubMed: 20675568]
52. Lakhkar A, Dhagia V, Joshi SR, Gotlinger KH, Patel D, Sun D, et al. 20-HETE-Induced Mitochondrial Superoxide and Inflammatory Phenotype in Vascular Smooth Muscle is Prevented by Glucose-6-Phosphate Dehydrogenase Inhibition. Am J Physiol Heart Circ Physiol. 2016;310(9):H1107–1117. Epub 2016/02/28. doi: 10.1152/ajpheart.00961.2015. [PubMed: 26921441]
53. Jiang M, Mezentsev A, Kemp R, Byun K, Falck JR, Miano JM, et al. Smooth muscle--specific expression of CYP4A1 induces endothelial sprouting in renal arterial microvessels. Circ Res. 2004;94(2):167–174. Epub 2003/12/13. doi: 10.1161/01.res.0000111523.12842.fc. [PubMed: 14670847]
54. Muntner P, Davis BR, Cushman WC, Bangalore S, Calhoun DA, Pressel SL, et al. Treatment-resistant hypertension and the incidence of cardiovascular disease and end-stage renal disease: results from the Antihypertensive and Lipid-Lowering Treatment to Prevent Heart Attack Trial (ALLHAT). Hypertension. 2014;64(5):1012–1021. Epub 2014/09/27. doi: 10.1161/hypertensionaha.114.03850. [PubMed: 25259745]

55. Williams JM, Murphy S, Burke M, Roman RJ. 20-hydroxyeicosatetraeonic acid: a new target for the treatment of hypertension. Journal of cardiovascular pharmacology. 2010;56(4):336–344. Epub 2010/10/12. doi: 10.1097/FJC.0b013e3181f04b1c. [PubMed: 20930591]

56. Wu CC, Gupta T, Garcia V, Ding Y, Schwartzman ML. 20-HETE and blood pressure regulation: clinical implications. Cardiol Rev. 2014;22(1):1–12. Epub 2013/04/16. doi: 10.1097/CRD.0b013e3182961659. [PubMed: 23584425]

57. Fan F, Muroya Y, Roman RJ. Cytochrome P450 eicosanoids in hypertension and renal disease. Curr Opin Nephrol Hypertens. 2015;24(1):37–46. Epub 2014/11/27. doi: 10.1097/mnh.0000000000000088. [PubMed: 25427230]

58. Pandey V, Garcia V, Gilani A, Mishra P, Zhang FF, Paudyal MP, et al. The Blood Pressure-Lowering Effect of 20-HETE Blockade in Cyp4a14(−/−) Mice Is Associated with Natriuresis. J Pharmacol Exp Ther. 2017;363(3):412–418. Epub 2017/09/16. doi: 10.1124/jpet.117.243618. [PubMed: 28912346]

59. Akbulut T, Regner KR, Roman RJ, Avner ED, Falck JR, Park F. 20-HETE activates the Raf/MEK/ERK pathway in renal epithelial cells through an EGFR- and c-Src-dependent mechanism. Am J Physiol Renal Physiol. 2009;297(3):F662–670. Epub 2009/07/03. doi: 10.1152/ajprenal.00146.2009. [PubMed: 19570883]

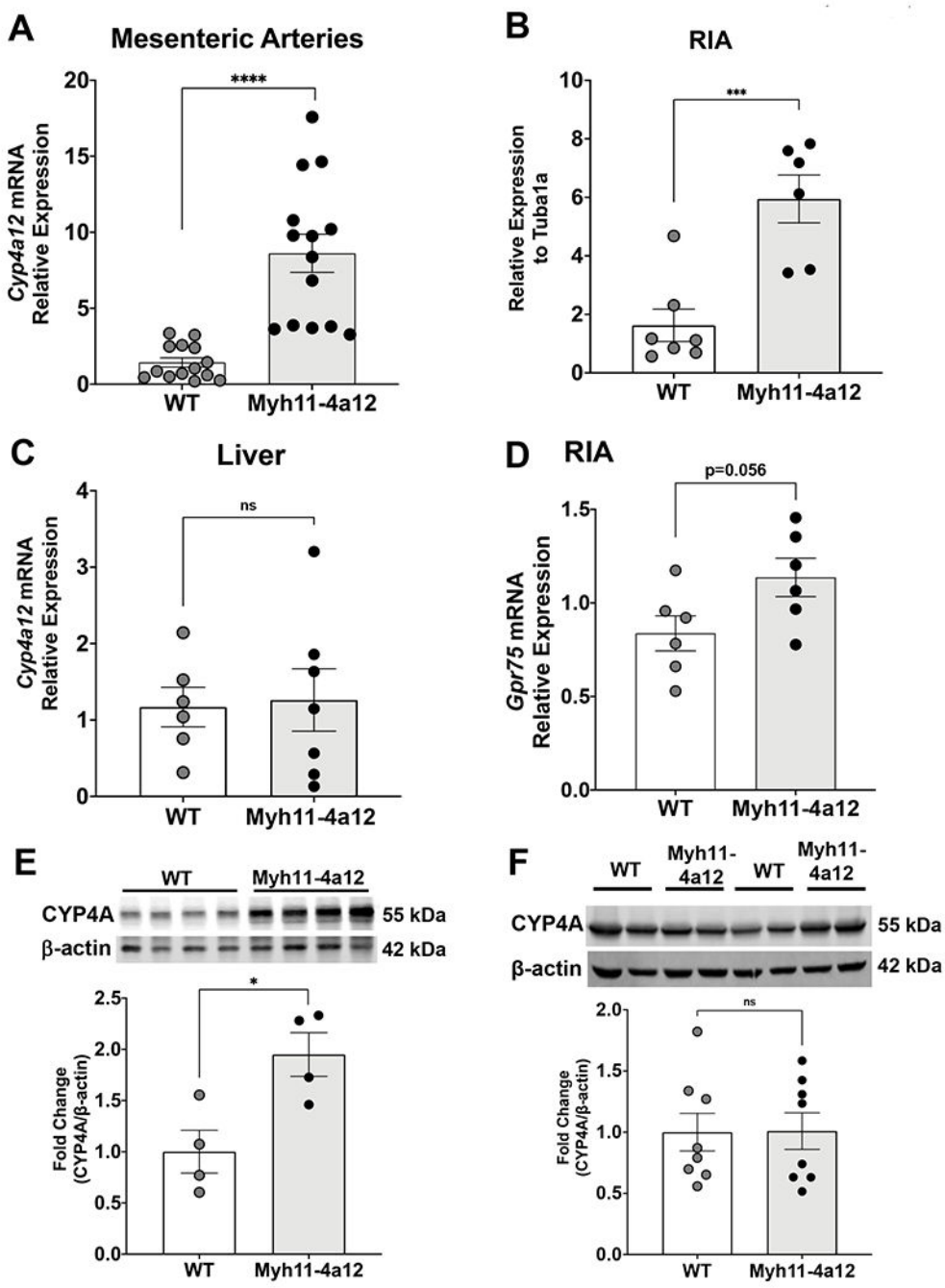

Figure 1:

Cyp4a12 mRNA levels in **A)** mesenteric arteries (N=14 mice/group), **B)** RIA (N=6 mice/group) and **C)** liver (N=6-7 mice/group). **D)** Levels of *Gpr75* mRNA in RIA (N=6 mice/group). CYP4A protein levels in **E)** mesenteric arteries (N=4 mice/group) and **F)** liver (N=8 mice/group). Results are means ± SE; *p<0.05, ***p<0.001, ****p<0.0001 vs. WT (unpaired t-test).

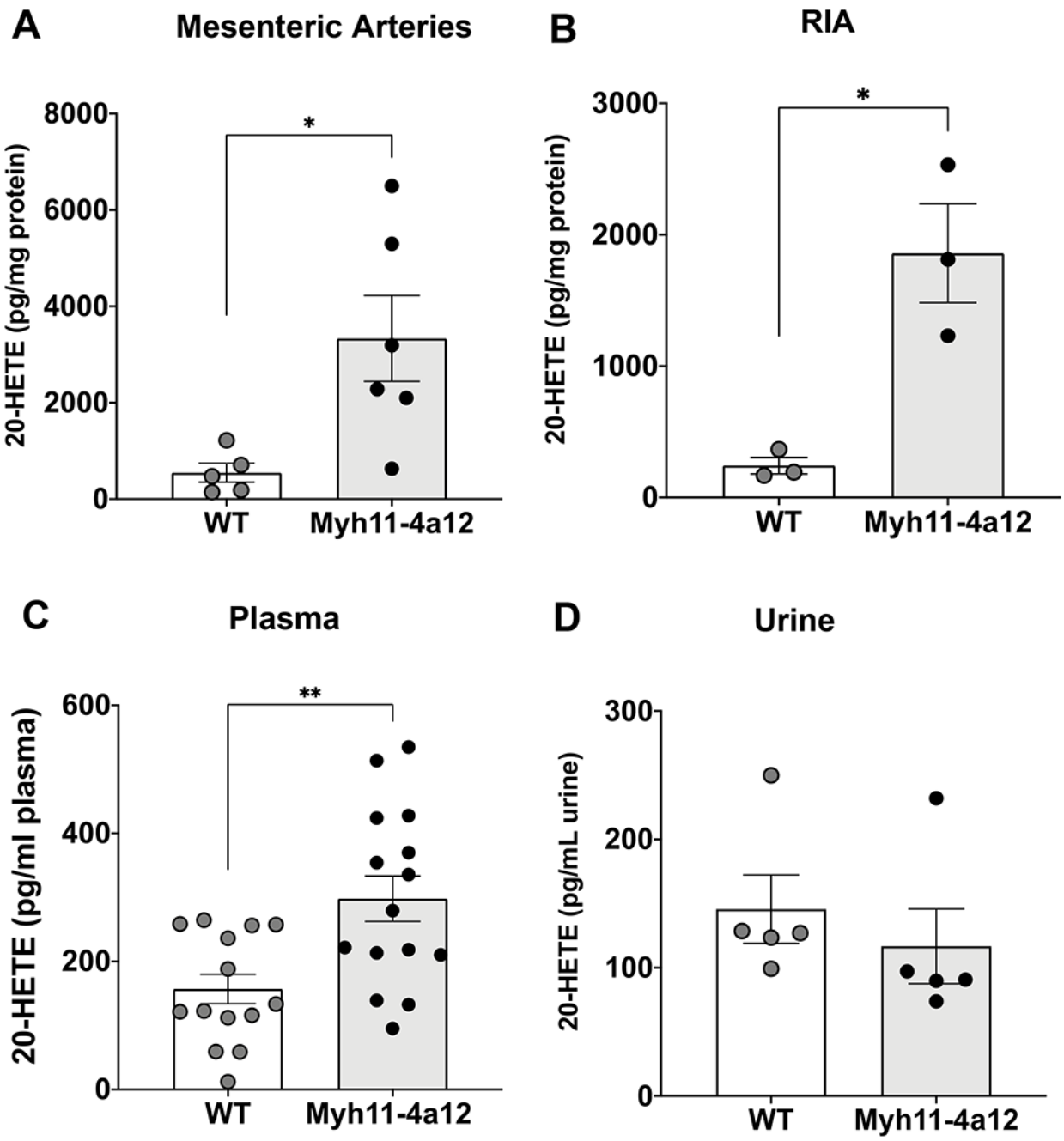

Figure 2:

20-Hydroxyeicosatetraenoic acid (20-HETE) levels in **A)** mesenteric arteries (N=5-6 mice/group), **B)** RIA (N=3 mice/group), **C)** plasma (N=14-15 mice/group), and **D)** urine (N=5 mice/group). Results are means ± SE; *p<0.05, **p<0.01 vs. WT (unpaired t-test).

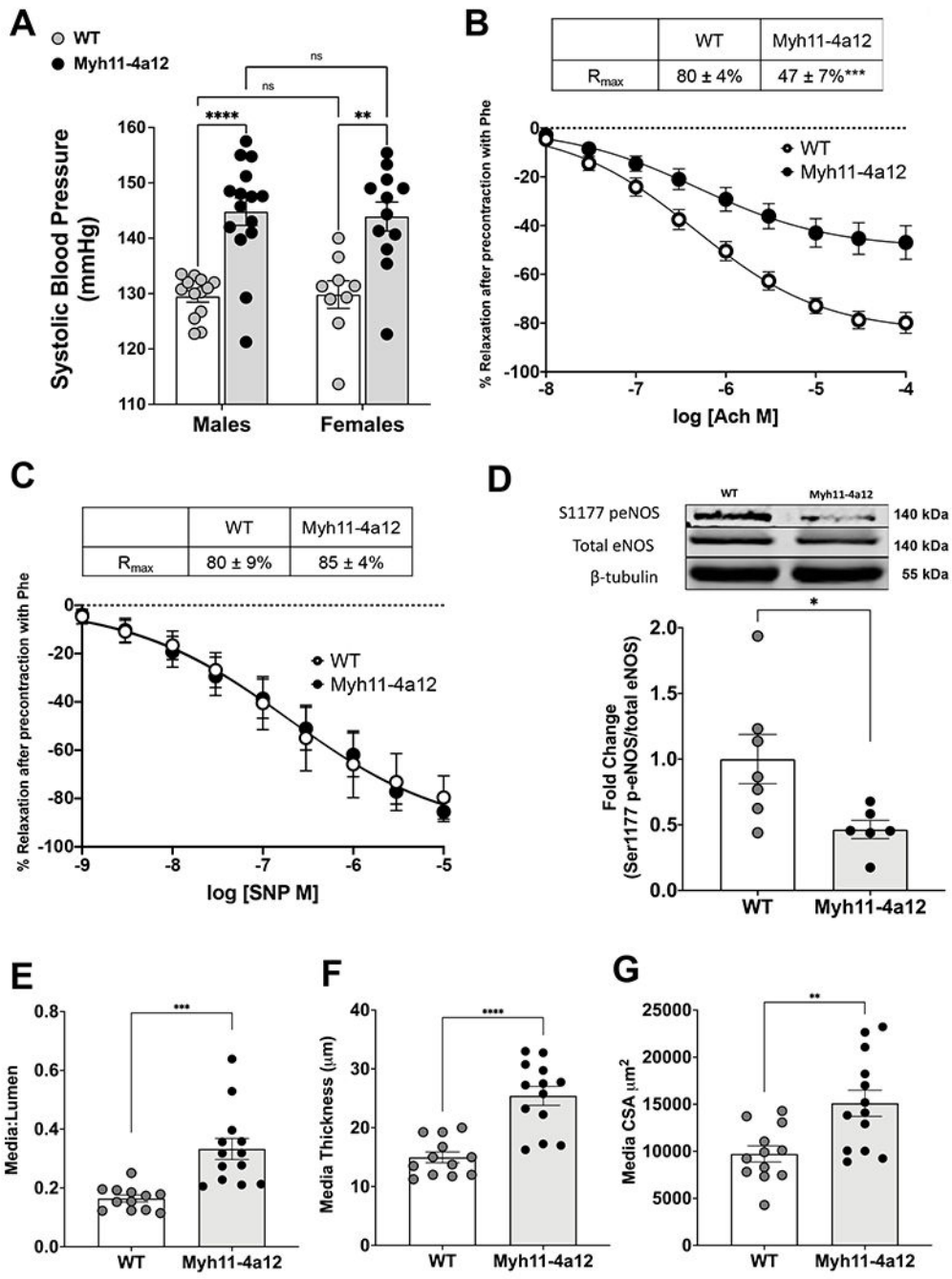

Figure 3:

A) Baseline systolic blood pressure in male and female mice (WT, M/F= 13/9; *Myh11-4a12*, M/F=15/12). Results are means ± SE; **p<0.01; ****p<0.0001 (2-way ANOVA). **B)** Baseline acetylcholine-induced relaxation in RIA (N=13 WT; N=15 *Myh11-4a12*). Results are means ± SE, ***p<0.001 (2-way ANOVA). **C)** Sodium nitroprusside (SNP)-induced relaxation in RIA (N=3 WT; N=4 *Myh11-4a12*). Results are means ± SE. **D)** Representative Western blot and densitometry analysis for Serine 1177 phospho-eNOS expression (N=6-7/group). Results are means ± SE; *p<0.05 (unpaired t-test). **E)** Media-to-lumen ratio, **F)**

media thickness and **G)** media cross-sectional area (CSA) (N=12-13/group) Results are means ± SE **p<0.01, ***p<0.001, ****p<0.0001 (unpaired t-test)

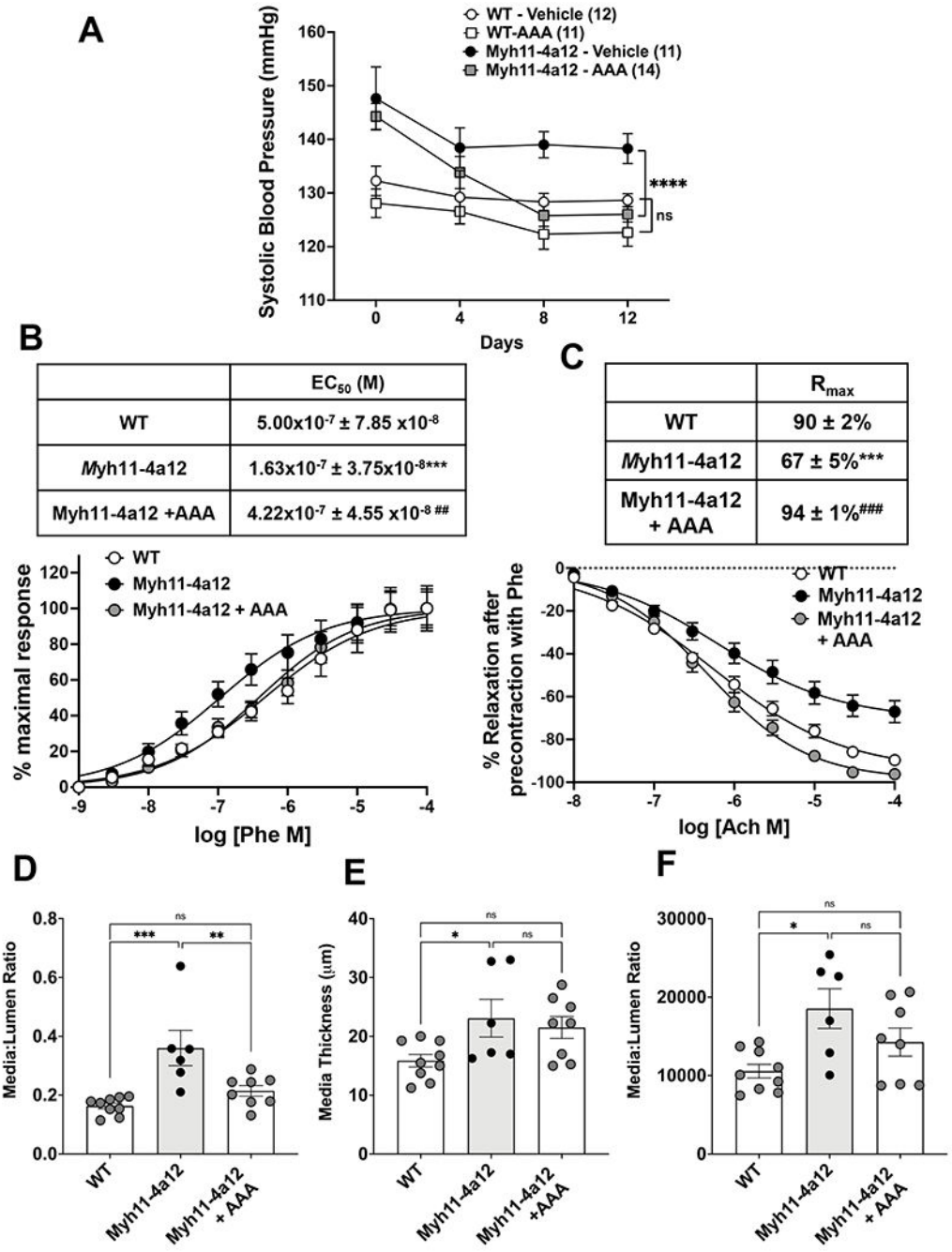

Figure 4:

A) Systolic blood pressure during 12 days of AAA treatment of WT and *Myh11-4a12* mice. Number of mice in each group is in parenthesis. Results are means ± SE, ****p<0.0001 vs vehicle-treated *Myh11-4a12* (2-way ANOVA repeated measures). **B)** Phenylephrine-induced contraction dose-response (N=7, WT; N=9, *Myh11-4a12*; N=6, *Myh11-4a12* + AAA). Results are means ± SE, ***p<0.001 vs WT; ##p<0.01 vs Myh11-4a12 (one-way ANOVA). **C)** Acetylcholine-induced relaxation dose-response (N=7 mice/group). Results are means ± SE, ***p<0.001 vs WT; ###p<0.001 vs vehicle-treated *Myh11-4a12* mice (one-way

ANOVA). **D)** Media to lumen ratio, **E)** media thickness, and **F)** media cross-sectional area (N=6-9/group). Results are means ± SE; *p<0.05, **p<0.01, ***p<0.001, ****p<0.0001 (one-way ANOVA).

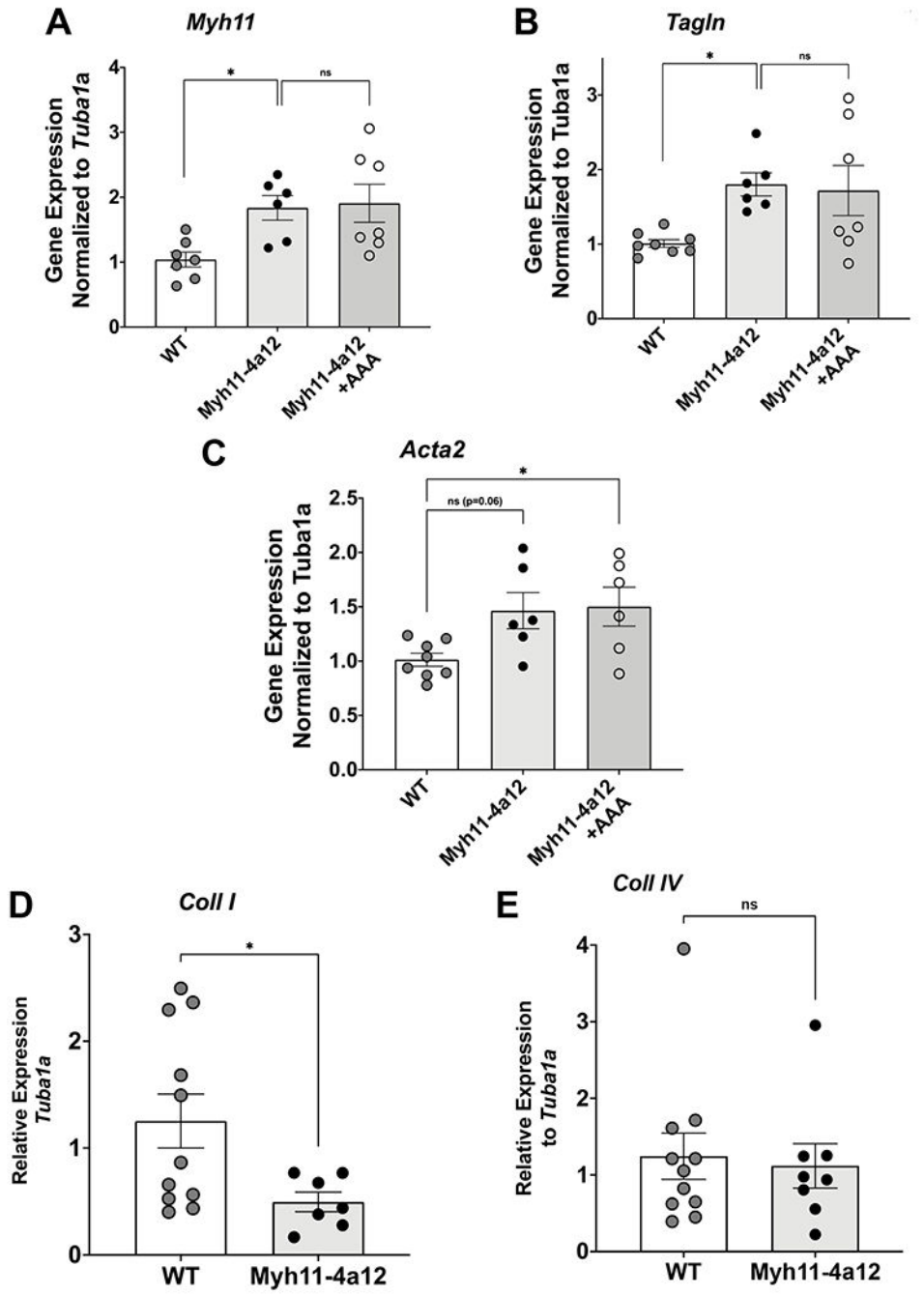

Figure 5:

Levels of mRNA in RIA arteries from wild type (WT), and vehicle- and AAA-treated Myh11-4a12 mice: **A)** *Myh11* (N=6-7 mice/group), **B)** *Tagln* (N=6-8 mice/group), **C)** *Acta2* (N=6-8 mice/group). Results are means ± SE, *p<0.05 vs WT (one-way ANOVA). Levels of mRNA in mesenteric arteries: **D)** *Coll I* and **E)** *Coll IV* in mesenteric arteries (N=7-11/group). Results are means ± SE, *p<0.05, (unpaired t-test).

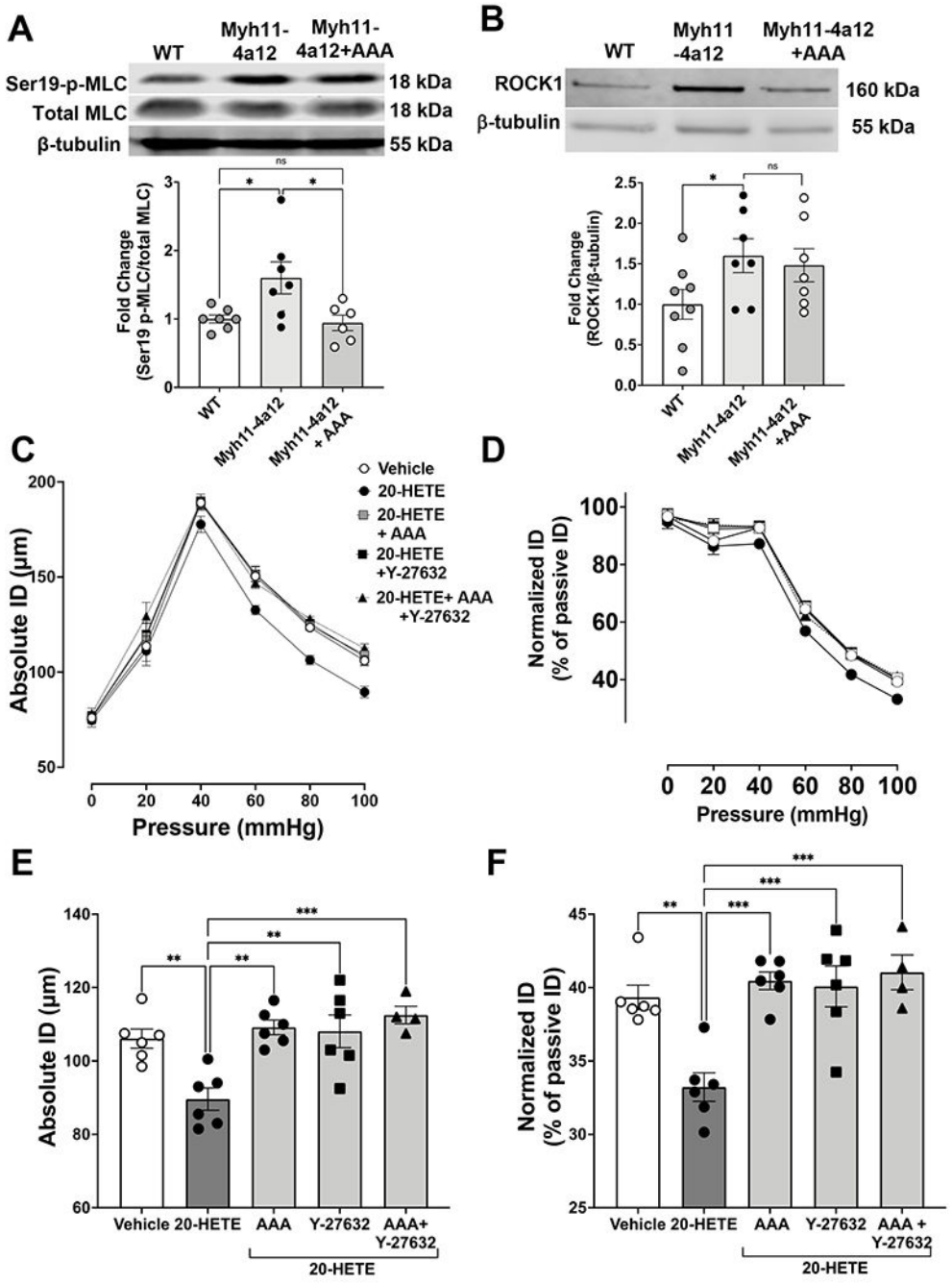

Figure 6:

A) Representative Western blots and densitometry analysis of phosphorylated myosin light chain phosphorylation (MLC) at serin 19 in mesenteric arteries. N=6-7/group). Results are means ± SE, *p<0.05 (one-way ANOVA). **B)** Representative Western blots and densitometry analysis of ROCK1 protein expression in RIA (N=7-8/group). Results are means ± SE, *p<0.05 (unpaired t-test). Myogenic response curve of RIA in response to 20-HETE (10 μM) with and without AAA (10 μM) and/or the ROCK inhibitor Y-27632 (10 μM) depicted as **C)** absolute internal diameter (ID) and **D)** normalized ID. Myogenic tone at 100 mmHg

depicted as **E)** Absolute ID and **F)** normalized ID (N=4-6/group). Results are means ± SE, *p<0.05, **p<0.01, ***p<0.001 (one-way ANOVA).